ORIGIN OF THE LUNAR CRUST INFERRED FROM MINERALOGY AND REFLECTANCE SPECTRA OF LUNAR METEORITES. T. Arai[1], T. Hiroi[2], S. Sasaki[3], and T. Matsui[1], [1]Planetary Exploration Research Center (PERC), Chiba Institute of Technology, 2-17-1 Tsudanuma, Narashino, Chiba 275-0016, Japan (tomoko.arai@it-chiba.ac.jp), [2]Department of Geological Sciences, Brown University, Providence, RI 02912, U.S.A., [3]RISE Project, National Astronomical Observatory of Japan (NAO), Mizusawa, Oshu, Iwate 023-0861, Japan.

Introduction: Lunar feldspathic crust is considered to be products of a primordial magma ocean crystallization. Distribution and composition of mafic minerals co-existing with plagioclase, such olivine and low-Ca pyroxene in the lunar crust are clues to understand the chemical composition and the mode of crystallization of a lunar magma ocean. Mineralogical analyses of the Apollo samples and previous remote sensing studies give us a general idea that the lunar crust is noritic where the abundance of low-Ca pyroxene far exceeds that of olivine [1, 2]. Accordingly, a magma ocean composition has been assumed to be saturated with low-Ca pyroxene and plagioclase [3]. On the other hand, recent mineralogical and geochemical studies of feldspathic lunar meteorites have revealed that olivine generally co-exists with plagioclase in the feldspathic clasts, suggesting that the lunar crust would be troctolic [4-6]. The Kaguya Spectral Profiler (SP) data show that olivine is present in the global crust, though its location is confined to basin rings and crater central peaks [7]. Co-existing anorthosite and troctolite on the Copernicus central peak is also reported by the Kaguya Multiband Imager (MI) data [8]. Thus, an understanding of true distribution of olivine and low-Ca pyroxene in the lunar crust is needed for proper understanding of a magma ocean composition and the lunar crustal genesis. In this study, occurrence, abundance and origin of olivine and low-Ca pyroxene in the lunar crust are discussed on the basis of mineralogy and visible-near infrared reflectance spectra of feldspathic lunar meteorites.

Samples and Methods: Three non-Antarctic feldspathic lunar meteorites DaG 400, Dhofar 908 and NWA 5000 were studied (Fig. 1). DaG 400 is a regolith breccia with a large troctolite clast of 2.3×2.0 cm in size. NWA 5000 is a fragmental breccias with mm-sized troctolite clasts. Dhofar 908 is a crystalline-matrix impact melt breccia with mm-sized clasts of anorthosite and troctolite. Bidirectional reflectance spectra in the wavelength range of 0.25-2.5µm were measured on the sliced chip surface of the above samples, with a Bunkoukeiki UV-Visible-NIR diffuse reflectance spectrophotometer in Mizusawa campus of NAO. The measurement geometry was set to 30° incidence and 0° emergence angles. Mineralogical analyses were performed on the above sliced surface of the samples, which were polished after the spectral measurement, with JEOL JSM-6510 LA analytical SEM at PERC, Chiba Inst. of Technology and JEOL JXA-8200 EPMA at National Institute of Polar Research of Japan.

Results: Troctolite clasts are present in a various type of feldspathic samples, such as regolith breccia (DaG 400), fragmental breccia (NWA 5000) and impact-melt breccia (Dhofar 908). Low-Ca pyroxene in these troctolite clasts generally occur as a minor phase. However, some troctolite clasts in Dhofar 908 show a slightly greater abundance of low-Ca pyroxene with unique occurrence. The low-Ca pyroxenes occur as an overgrowth of olivine in the grain boundary between olivine and plagioclase, showing a corona-like texture (Fig. 2).

The greater abundance of low-Ca pyroxene in the Dhofar 908 troctolite clasts is also recognized among reflectance spectra of the three samples (Fig. 3). Spectral features of olivine-rich areas of DaG 400 and NWA 5000 (DaG400_3, NWA5000) (Figs. 1, 3) display absorption bands around 1.05 µm, which is diagnostic of olivine. In contrast, those of Dhofar 908 (Dho908_3) show absorption band around 0.9 µm, which is diagnostic of low-Ca pyroxene, instead of olivine absorption around 1.05 µm. Even though the modal abundance of olivine much exceeds that of low-Ca pyroxene in the Dhofar 908 troctolite clast (Fig. 2), the presence of olivine is masked by minor presence of low-Ca pyroxene in the reflectance spectral data. Note that reflectance spectra of plagioclase-rich areas (DaG400_1, Dho908_1)(Figs. 1, 3) shows broad absorption band around 1.25 µm, which is diagnostic of plagioclase.

Discussion:

Lower survivability of olivine: The corona-like low-Ca pyroxnes in the Dhofar 908 trocotlite clasts show that low-Ca pyroxenes do not form by a simple monotonic cooling of magmas, but by a reaction between disequilibrium pairs of olivine and SiO_2-rich melt. The partial replacement of olivine by low-Ca pyroxene is controlled by a peritectic reaction between the two phases, as shown by an equation below:

$$\underset{\text{Olivine}}{(Fe,Mg)_2SiO_4} + \underset{\text{Melt}}{SiO_2} \rightarrow \underset{\text{Low-Ca pyroxene}}{2*(Fe,Mg)SiO_3}$$

Considered the above occurrence of low-Ca pyroxene, and a peritectic relation between low-Ca pyroxene and olivine, low-Ca pyroxene in the lunar feldspathic rock likely formed during the secondary metamorphism of the olivine-bearing primary igneous crust. The texture of olivine, low-Ca pyroxene, and plagioclase indicates that olivine crystallizes first, followed by plagioclase crystallization, and subsequently low-Ca pyroxene forms in between the two minerals either during the later course of crystallization or secondary heating after the completion of crystallization.

Lower detectability of olivine: Olivine is detected by the Kaguya MI and SP in the global crust, but the abundance is still far lower than that of low-Ca pyroxene [7]. The apparent lower abundance of olivine relative to low-Ca pyroxene in the feldspathic crust seems inconsistent with the general presence of troctolite clasts in the feldspathic lunar meteorites. This contrast may be attributed to the lower detectability of olivine compared with pyroxene, due to the absorption coefficient of olivine which is by far smaller than that of pyroxene in a visible to near-infrared wavelength [e.g. 9]. The absorption of olivine in the reflectance spectra can be easily masked by that of pyroxene, when the two minerals coexist. Thus, the locations where olivine is detected by the SP are exclusively rich in olivine with or without plagioclase.

The presence of olivine is limited to relatively fresh craters on basin rings and crater central peaks [7]. Cratering mechanism studies show that basin rings and crater central peaks tend to represent uplifted deep-seated crustal rock, with little heating and melting. In such locations, the primary olivine can survive, and thus the initial crust composition consisting of olivine and plagioclase is likely preserved without the secondary metamorphism.

Mineralogical studies of feldspathic lunar meteorites show that low-Ca pyroxenes are likely the secondary product after olivine and plagioclase crystallized from a magma. The fact suggests that plagioclase and olivine be the two dominant minerals in the initial crust which formed by a magma ocean crystallization, but low-Ca pyroxene may not be a direct product from a magma ocean. If that is a case, a magma ocean composition needs to be more aluminous than that previously estimated by a factor of two or three [10]. Replacement of the primary olivines by low-Ca pyroxenes during the secondary heating events, such as multiple impacts and subsequent volcanic activities after the magma ocean solidification may have altered an initial abundance of olivine in the primary crust. Lower detectability of olivine than low-Ca pyroxene in the reflectance spectra observation may further bias the real abundance of olivine in the present lunar crust.

References: [1] Hawke B. R. et al. (2003) JGR 108, DOI:10.1029/2002JE001890. [2] Lucey P. G. (2004) GRL 31, L08701. [3] Longhi J. (2003) JGR 108, doi:10.1029/2002JE001941. [4] Korotev R. L. et al. (2003) GCA 67, 4895-4923. [5] Korotev R. L. et al. (2006) GCA 70, 5935-5956. [6] Takeda H. et al. (2006) EPSL 247, 171-184. [7] Yamamoto S. et al. (2010) Nature geosciences 3, 533-536. [8] Arai et al., (2011) LPS XXXXII, #2379. [9] Pieters C. M. and P. A. J. Englert (Eds.) (1993) Remote Geochemical Analysis: Elemental and Mineralogical Composition, 594 pp., Cambridge University Press, Cambridge. [10] Warren P. H. and Wasson J. T. (1979) PLPSC 10th, 2051-2083.

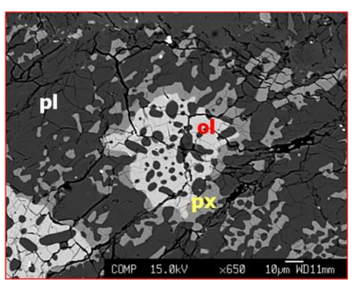

Fig. 2 BSE image of an overgrowth of low-Ca pyroxene on olivine in Dhofar 908 troctolite clast. Ol: olivine, px: pyroxene, pl: plagioclase (FOV: 0.2 mm).

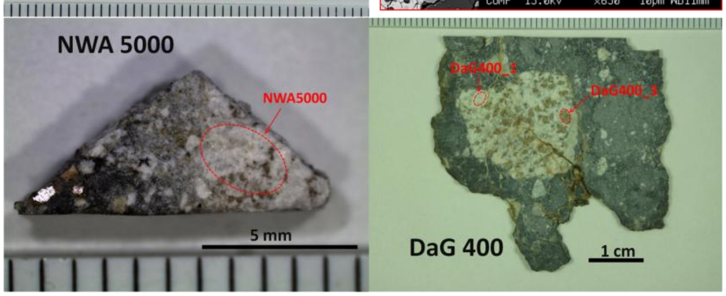

Fig. 1. Photomicrographs of the three feldspathic lunar meteorites with troctolite clasts. Red circles indicate measured spots (about 3×2 mm in size) for reflectance spectral analyses.

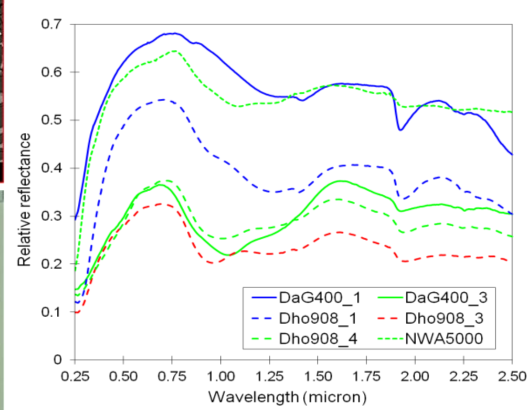

Fig. 3. Reflectance spectra of troctolites in the three samples. Blue spectra is plagioclase dominated, green ones are olivine dominated, and a red one is low-Ca pyroxene dominated, in the reflectance spectral viewpoint.